ELSEVIER

Colloids and Surfaces A: Physicochem. Eng. Aspects 263 (2005) 52–64

COLLOIDS AND SURFACES A

www.elsevier.com/locate/colsurfa

Rheology of ordered foams—on the way to Discrete Microfluidics

W. Drenckhan[a,*], S.J. Cox[a,1], G. Delaney[a], H. Holste[a], D. Weaire[a], N. Kern[b]

[a] *Department of Physics, Trinity College Dublin, Dublin 2, Ireland*
[b] *Laboratoire des Colloides, Université Montpellier II, Montpellier, France*

Received 7 October 2004; accepted 12 January 2005
Available online 19 February 2005

Abstract

Microfluidics is a rapidly developing field of innovation, which provides the chemical, medical and (bio)pharmaceutical industries with a much more efficient substitute for the use of well plates, syringes, etc., to perform multiple manipulations and analysis of small samples. While conventional, continuous microfluidics and the manipulation of individual nano-droplets in "Digital Microfluidics" are highly advanced, a major new dimension is added by our work on the flow of ordered foam and emulsion structures in specifically designed channel geometries. We show experimentally and computationally, utilizing both the quasi-static and Viscous Froth models, how the interplay between channel geometry and ordered foam/emulsion structures can be used to process tiny amounts of gases or liquids in a highly reliable and efficient way. We have termed this method "Discrete Microfluidics" and will introduce its various aspects in this paper.

Keywords: Rheology; Viscous Froth models; Discrete Microfluidics

1. Introduction

The handling of small quantities of liquids and gases has moved into the focus of various technological fields, ranging from pharmaceutical, medical and biological applications to printing. Many of its challenges are met by quickly advancing microfluidic technologies [1–8], which utilize an assembly of micro-channels and detectors on small chips to manipulate liquids by various means. These *Total Analysis Systems* are at the verge of replacing traditional macro-sized labs with *Labs-on-a-Chip* [1,9,10], which contribute to an extraordinary down-scaling of spatial and financial requirements in a plethora of fields. However, even though the field of microfluidics has seen astonishing leaps in its development in recent years, important issues remain unsolved and have proven to be very difficult to tackle within the framework of traditional methods [2,11].

New advances have been made in using individual droplets, rather than continuous liquids, for the purpose of controlled transport and mixing. This method was termed *Digital Microfluidics* [12].

With our background in the physics of foams, we take the digital approach an important step further by utilizing the manipulation of ordered foam and emulsion structures in specifically designed channel geometries. An illustrative example is shown in Fig. 1, where an ordered foam structure of two rows of samples is split into two separate individual rows by pushing it through a Y-shaped channel on a chip.

The possibility of sorting the discrete cells of a two-phase system purely by moving the samples through specific channel geometries is a result of one of the most fundamental physical principles: minimization of energy. At low flow velocities the energy of a two-phase system is well represented by its interfacial area and therefore by its structure [13]. For higher flow velocities, the viscous dissipation between the foam/emulsion and the channel walls becomes increasingly important and has to be included in the energy balance (see Section 5).

By trapping foams or emulsions in channels of purpose-designed geometries, specific boundary conditions are forced upon the two-phase system, which act to select particular sample arrangements. As the samples move through the channel, their structure undergoes well-defined transitions, which

* Corresponding author. Tel.: +353 1 6082157; fax: +353 1 6711759.
E-mail address: Wiebke.Drenckhan@tcd.ie (W. Drenckhan).
[1] Present address: Institute of Mathematical and Physical Sciences, University of Wales Aberystwyth, SY23 3BZ, UK.

0927-7757/$ – see front matter © 2005 Elsevier B.V. All rights reserved.
doi:10.1016/j.colsurfa.2005.01.005

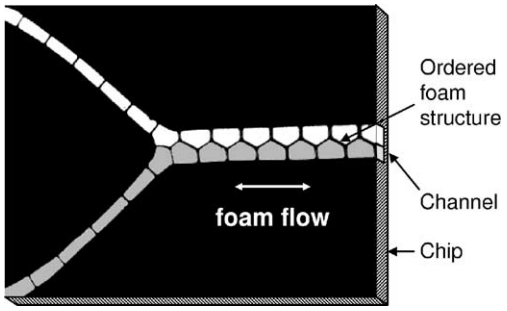

Fig. 1. Example of the flow of ordered foam structures in a quasi-2D channel geometry. A Y-shaped channel can be used to split rows of bubbles.

can be utilized for sample manipulation in various ways (see Section 4).

This method, which we have termed *Discrete Microfluidics*, has many advantages over current practice, of which some of the most striking are:

- Since Discrete Microfluidics is based on the minimization of interfacial area, the samples can either be gaseous (foam) or liquid (emulsion) for the same channel geometry.
- If diffusion between the sample is prohibited, an indefinite number of them can be treated on the same chip.
- As most of the sample manipulation is based on pure geometry, the number of movable (and hence sensitive) parts on a chip can be greatly reduced.
- Due to the discrete nature of the method, sample manipulation becomes very reliable and quantifiable. Samples can be labeled and traced easily throughout the chip.
- The minimization of interfacial area of a structure can be modeled more easily than the complex fluid dynamics of continuous (micro)fluidic processes. Hence, a major part of the channel design can be done by computer simulation, rather than expensive trial and error experimental procedures (see Section 4.1).
- A well-know problem of traditional microfluidics is the lack of an efficient link between the micro-chip, the micro-arrays (well plates) and sample storage. Our technology unifies these in a straightforward way (see Section 6).
- If the sample material is chosen such that it makes up a small volume fraction of the two-phase system, the sample material can be greatly reduced whilst maintaining reasonably large channel sizes. This is particularly interesting for analysis methods requiring the use of solid particles (beads), which would clog up small channels.

Arranging the various channel elements in a network, which integrates sample generation, analysis and storage, provides a straightforward way of designing Total Analysis Systems.

Another dimension of manipulation is added by using magnetic fluids and appropriately designed magnetic fields. These can be utilized for

- generation and magnetic manipulation of ferrofluid foam structures [14];
- precise bubble size control by applying magnetic field gradients during bubble generation in a ferrofluid [15];
- detection of films and measurement of bubble volumes using local conductivity measurements [15].

In this article we focus on the rheology of ordered two-phase structures in various confining geometries, combining experiments and computer simulations. At the outset we give a brief introduction to ordered foam structures (Section 2) followed by a description of the experimental set-up and procedure.

The simulations and experiments considered here are of two-dimensional (2D) and quasi-2D nature, respectively. Experimentally this is achieved by working with channel systems in which one of the length scales is significantly smaller than the other two. In our case this provides a system comprised of mono-layers of bubbles or droplets, which has many advantages over true three-dimensional systems. Not only does it significantly simplify the observation, analysis and modeling, but it is more straightforward to manufacture with lithographic, stamping or carving techniques.

Most of the experiments described here can be successfully modeled by considering them to be in the quasi-static regime, as demonstrated in Section 4 by comparing experiments and computer simulations. However, aiming for high sample throughput in applications demands the consideration of viscous effects in foam rheology. In Section 5 the viscous drag of foam films along the channel walls at high foam flow velocities is taken into account by modelling the flow with the “Viscous Froth Model” [16]. Despite its simplicity, this model has proven highly successful in reproducing the experimental observations.

All investigations reported here were conducted on the millimeter scale. It remains to be seen how easily the principles introduced here can be applied on the length scales required by microfluidics. Initial experiments on ordered micro-emulsions [17] and micro-foams [18] have been very successful. We would like to emphasize, however, that not every promising application requires microfluidic dimensions. Even on millimeter scale we envisage interesting opportunities, for instance in the production of medical pills, the analysis of environmental gas samples or blood samples.

After Section 2 we will only talk about foams and bubbles, as most of our experiments have been conducted with these. The reader should keep in mind, however, that the introduced methods should equally apply to emulsions and droplets [19].

2. Ordered foam and emulsion structures

Due to their complex energy landscapes, foams are generally highly disordered. However, if bubbles of equal volume are introduced into regular containers of cross-sections of the order of a few bubble diameters, they arrange in a highly

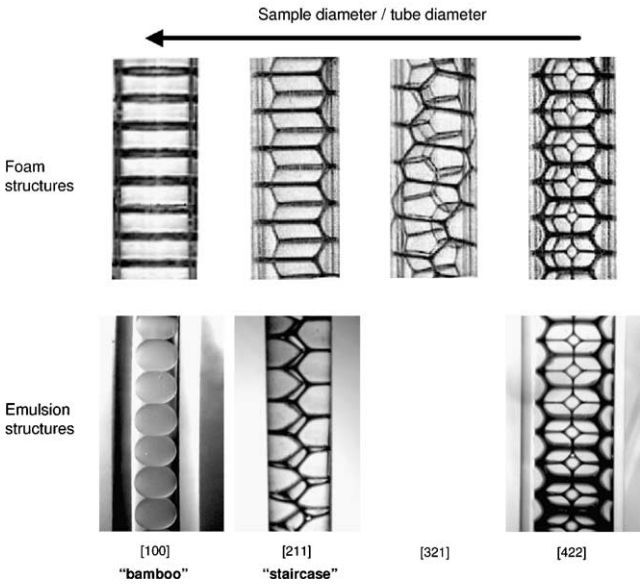

Fig. 2. Ordered foam and emulsion structures in cylindrical tubes. The topology of the periodic bubble arrangement depends on the ratio of the bubble (droplet) diameter to tube diameter. (The emulsion consists of silicone oil in water stabilized by "Fairy liquid" dish washing solution.)

ordered and predictable manner [20–22,14]. Fig. 2 shows photographs of some simple cases of these structures generated with foams and emulsions in cylindrical tubes. The specific topology of the periodic bubble arrangement depends on the ratio of the tube diameter to the bubble or droplet diameter. Computer simulations using the Surface Evolver [23] successfully reproduce these patterns [13].

Classification of these structures is achieved by employing the (cylindrical) phyllotactic notation $[i,j,k]$ of the hexagonal pattern formed on the surface of the container [20].

In two-dimensional systems these ordered structures reduce to i columns of bubbles, which we classify with the notation $[i]$. Fig. 3 shows an experiment of a series of highly localized transitions between consecutive structures of a mono-disperse foam continuously flowing through a wedge-shaped, quasi-2D channel (transitions: [1] → [2] → [3] → [2] → [1]). The experimental set-up is described in more detail in Section 3.

The image displays a very strong hysteresis between the $[i]$ → $[i+1]$ and the $[i+1]$ → $[i]$ transition. The ratio of bubble

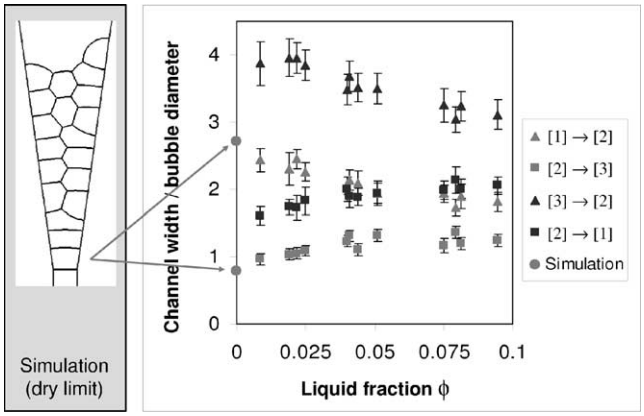

Fig. 4. Experimental data showing the ratio channel width/bubble diameter as a function of liquid fraction for the wedge-shaped quasi-2D channel displayed in Fig. 3. Computer simulations for the perfectly dry foam fit very well to the data.

diameter to channel width at which the transitions occur, and the magnitude of the hysteresis, depends very much on the liquid fraction of the foam. The wetter the system is, the less hysteresis plays a role, as the foam can explore its energy landscape more easily. A similar system has been investigated for wet foams by Rosa and Fortes [24].

Fig. 4 shows experimental data of the channel width to bubble diameter ratio for the transitions shown in Fig. 3 for various liquid volume fractions. It is clear that the amount of liquid in the foam structure has a significant effect on the ratio at which these transitions occur. Computer simulations for the dry limit ($\phi = 0$), using the Surface Evolver [23], fit very well to the experimental data.

A thorough understanding of these transitions is crucial for a successful application of Discrete Microfluidics. In order to manipulate and analyze samples and sample structures in networks of channels, it is important to be able to predict and control the type of structure present at any point in the network.

3. Experimental set-up and procedure

Here we work with quasi-2D systems of typically 0.5–1.5 mm channel depth and up to 10 mm channel width. For exploratory investigations these channels are created us-

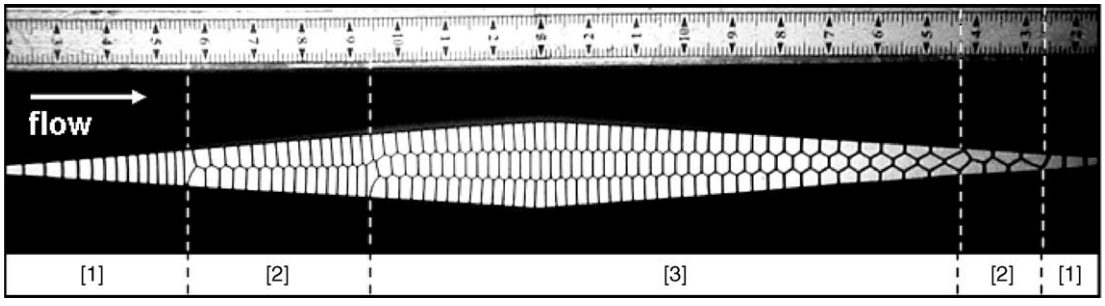

Fig. 3. Transitions between ordered 2D foam structures as a result of foam flowing through a quasi-2D, wedge-shaped channel.

ing a simple "sandwich" system of a plane rubber sheet between two glass plates. Channels of arbitrary shape can easily be cut into the sheet using, for instance, a sharp razor blade. This leads to the side walls of the channel being a rubber surface and the top and bottom wall being glass surface.

For quantitative investigations, the channel geometries are designed in Autocad and then carved into a plane Plexiglas sheet. This is glued onto another plane Plexiglas sheet in order to close the channel system. In these types of channels all walls are Plexiglas, which provides constant surface properties throughout the system (Series S402).

Bubbles of equal volume are generated by injecting nitrogen gas into Fairy Liquid-dish-washing solution of 0.4% concentration. We use nitrogen gas because of its low diffusivity in water, which greatly reduces the coarsening of the foam [13]. The bubbles are collected in a vertical capillary, diameter of which is chosen such that the bubbles arrange in a "staircase" structure (see Fig. 2) [20]. This is because unlike the "bamboo" structure (see Fig. 2), the staircase structure allows liquid to drain easily. We use this in order to set the liquid volume fraction in the foam by applying forced drainage [13] at the top of the capillary. Once the volume fraction is set, the capillary is quickly moved into a horizontal position to avoid further drainage. Choosing the capillary radius as small as possible reduces the amount of vertical drainage in the foam while it is held horizontal. The horizontal capillary is placed between a pressure supply and the channel system. This foam is then driven through the channel system by applying a constant gas (nitrogen) pressure at the inlet. For a sketch of the set-up see Fig. 5.

Images are recorded with a digital camera. The best image quality is achieved by placing the horizontal, transparent channel system between a diffusive, bright light source and the camera. Due to the curved nature of the interfaces the films and vertex boundaries appear black in the images. The bottom part of an overhead projector covered with a diffusing sheet has proven to provide the most homogeneous lighting.

The reader should keep in mind that surface Plateau borders are formed wherever films are attached to the channel walls. This not only has an effect on the apparent film thickness, but also on the flow properties of the foam. It is a 3D-effect and can be neglected for most of the cases considered here. For higher flow velocities, however, it has to be taken into account (see Section 5) [26].

4. Quasi-static foam rheology in confined geometries

We showed in Section 2 that the structure of an ordered foam is determined by its confining geometry. Hence, by designing channels or containers of specific geometries, we can not only control the structure of the foam, but we can use it to perform "logic operations" on the bubbles as the structure flows through these channel elements.

In the following we give a brief introduction to the quasi-static computational modeling employed for low foam flow velocities, before demonstrating how simulation and experiment are combined in some examples of channel elements. These should be thought of as individual "building blocks" for a more complex network of channel geometries performing specific tasks of bubble manipulation.

4.1. Computational modeling

Computer simulations are vital for the efficient design of channel systems and to test our physical models of foams and foam flow. For many of our purposes it is sufficient to apply 2D simulation [27].

Simplification can be taken further by modeling perfectly dry foams. In such a system, films are represented by lines (edges) and vertices by the points at which these edges meet. The wetness of the foam can then be accounted for by adjusting the critical edge-length at which neighbor-switching

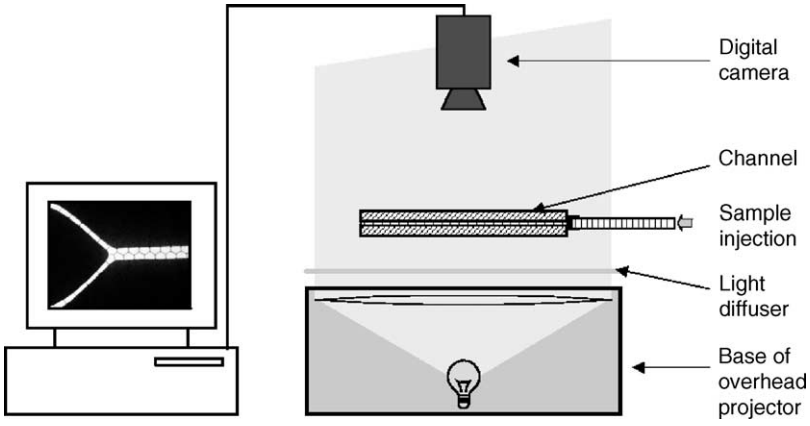

Fig. 5. Setup for 2D-foam rheology: Quasi-2D channels are carved into a Plexiglas sheet, which is then glued onto another plane Plexiglas sheet. Monodisperse bubbles are injected into the horizontal channel system from a capillary by applying a constant gas pressure. The system is lit from below with an overhead projector topped with a light-diffusing sheet. Images and videos are recorded with a digital camera from above and subsequently analyzed on the computer using ImageJ [25].

processes between bubbles occur. The wetter the foam, the longer this critical length.

For reasonably low flow velocities we can assume quasi-static flow, whereby simulations proceed by a process of small increments in position and energy minimization, allowing the foam structure to move via a sequence of equilibrium states. This can be done with the software package Surface Evolver developed by Brakke [23]. The required 2D foam structure is pushed through the channel in this way boundaries. After each step the total line length (energy) of the system is minimized, whilst keeping the bubble volumes constant.

For low flow velocities this procedure has proven very successful in reproducing the experimental observations. For higher velocities, however, viscous drag acting on the surface Plateau borders has to be taken into account. The magnitude of the critical velocity at which the quasi-static approach breaks down and the flow becomes dominated by viscous forces depends on various parameters, of which the most important are the liquid fraction and the channel depth. Much of the work reported in Section 5 attempts to explore this dependence.

4.2. The Y-junction

Branching channels can be used to maneuver bubbles into different parts of a network or to (re)combine them. The ratio of the channel widths of the branches determines the "sorting algorithm".

An example is demonstrated in Fig. 6(a), where one channel containing two rows of bubbles is split into two channels containing one row of bubbles each. Fig. 6(b) shows an image of a computer simulation for this device.

These processes are perfectly reliable and reversible. The reversibility is demonstrated in Fig. 6(c). Here a double row of bubbles is split into two individual ones, which are then recombined to form the same double row structure as initially present. This type of channel could furthermore be used to introduce a well-defined phase shift between the two rows of bubbles by choosing an appropriate length difference between the two separate branches.

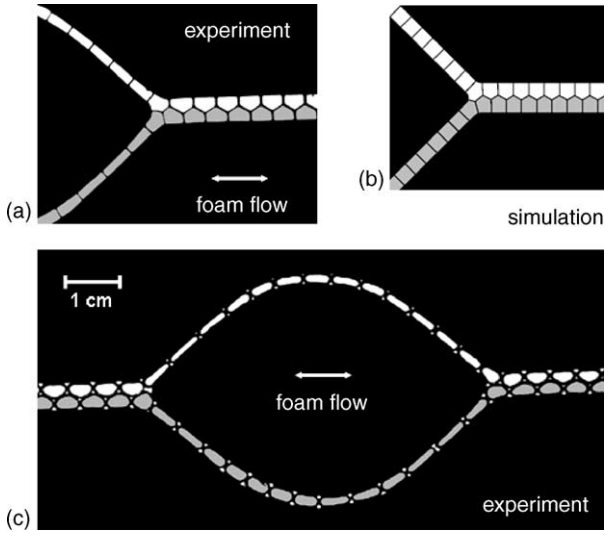

Fig. 6. The Y-junction. (a) Experiment and (b) simulation of a channel geometry which divides a structure of two rows of bubbles into two structures containing one row of bubbles each. The reversibility of this process is demonstrated in (c).

4.3. The flipper

Specifically designed local narrowings or bulges in a channel can make use of consecutive transitions between structures to re-arrange bubbles within one channel. Fig. 7 shows experiments and simulations of two typical examples in which one or two "Gaussian bumps" cause a [2] → [1] → [2] transition, during which the bubbles are re-arranged so that the two rows of bubbles switch sides in the channel.

Care has to be taken in choosing the initial configuration of the staircase structure. When the foam flow is set up, one of the bubble rows will be in advance of the other by one bubble at the very beginning of the foam structure. Depending on whether or not this is the first row which hits the "bump", the channel element may or may not switch them. More thought will have to go into a design that will work independently of this initial condition.

4.4. The magic cross

Bubbles can easily be added, removed or replaced in a structure using T-junctions or intersections of channels with individually controlled flow/pressure.

An example of a very versatile device is demonstrated in Fig. 8. Two intersecting channels contain a single row of bubbles each. The main flow occurs in the horizontal channel from left to right. If the top of the vertical branch is closed (so that the system is equivalent to a T-junction), appropriate pressure pulses or pressure drops applied to the bottom

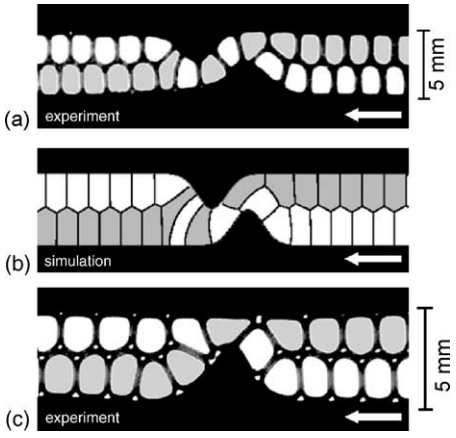

Fig. 7. The Flipper. (a) Two "Gaussian bumps" or (c) one in a channel can be used to provoke controlled [2] → [1] → [2] transitions, which result in a re-arrangement of the bubbles such that the two rows of bubbles are switched within a single channel. (b) is a computer simulation of the experiment shown in (a).

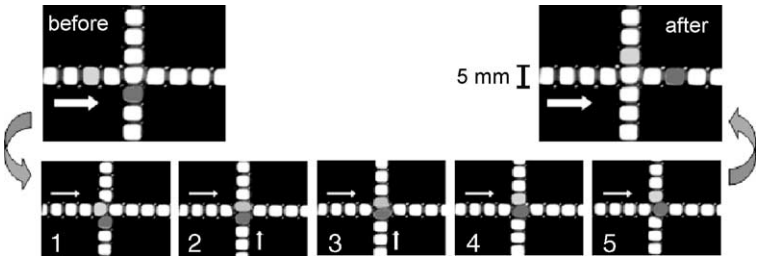

Fig. 8. The magic cross. Two crossing channels each contain a single row of bubbles. The bubbles in the horizontal channel flow continuously. Upon the application of an appropriate pressure pulse in the vertical channel, a bubble from the horizontal channel (light gray) can by replaced with a bubble (dark gray) from the vertical channel.

branch result in the controlled injection or removal of bubbles to/from the main channel. If the top branch is open, as in the example shown in Fig. 8, a well-timed pressure pulse results in a bubble from the main channel (light gray) being replaced by a bubble from the crossing channel (dark gray).

Devices of this type could be used to inject tracer bubbles in a network, or to remove "bad" bubbles which failed a test at a detector. Moreover, they could be used to construct specific sequences of bubbles containing different chemical substances. A controlled breaking of films at a later stage could provoke chemical reactions or the mixing of minute quantities of gases or liquids.

4.5. Around the bend

The flow around a tight bend exerts a localized shear on the staircase structure, which can be used to induce one or more neighbor-switching processes between adjacent bubbles. If applied continuously, this results in an effective phase shift of the bubble rows; i.e. the inner row is shifted with respect to the outer one.

Fig. 9 demonstrates an example in which one neighbor switching process is trapped in a U-bend: the gray bubbles are initially separated by two white bubbles which touch each other. Going through the bend reverses this configuration such that the white bubbles become separated by the pair of touching gray bubbles. All the following bubbles are switched in the same way, which introduces a phase shift of one bubble between the two rows.

Unlike in the other devices it is not sufficient to employ quasi-static modeling for a full understanding of the functioning of this device. The initial switching process is triggered by the local shear of the sample structure, which is induced by the viscous drag on the walls and hence depends on the flow velocity. In order to tackle this problem we use the Viscous Froth Model [16], which has proven very successful in reproducing experimental observations. In this context we revisit the U-bend device, among others, in Section 5, giving a more extensive discussion of the physics governing the operation of this device and the related modeling.

5. Viscous foam flow

In order to meet the industrial requirements of high sample throughput on a Lab-on-a-Chip, it will be important to consider the effect of high flow velocities in the devices introduced in the previous sections.

Effects of the channel walls will become increasingly important compared to bulk effects as we go down to smaller length scales. At high flow velocities, an increasingly dominant contribution is expected from the viscous dissipation of

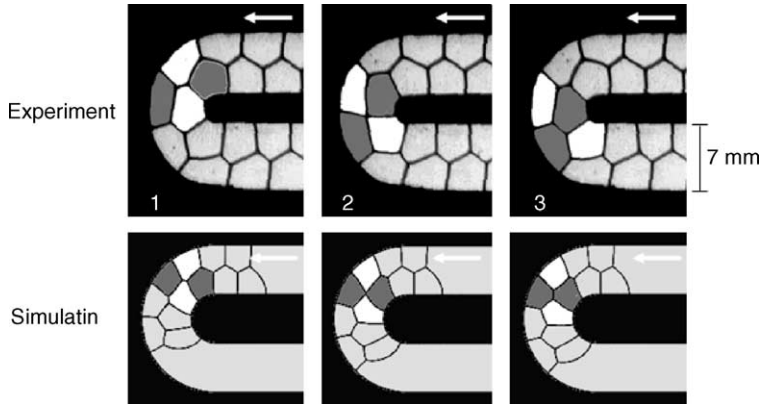

Fig. 9. Around the bend. (a) Experiment and (b) computer simulation of the neighbor switching process using the Viscous Froth Model, introduced in Section 5. The neighbor switching process generates a phase shift of one bubble between the two bubble rows.

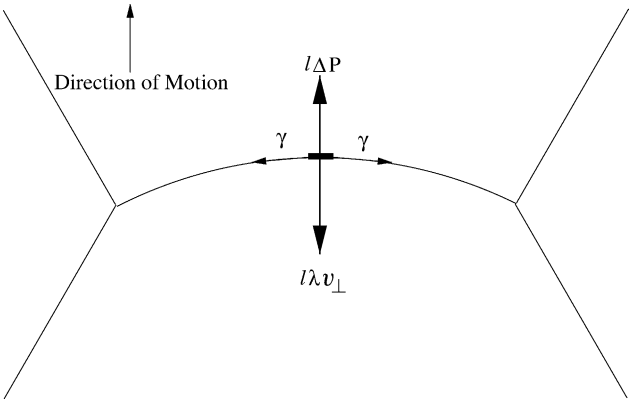

Fig. 10. Forces acting on a film segment of length l in the Linear Viscous Froth Model (Eq. (5.1) with $\alpha = 1$). The dissipative force that opposes motion is proportional to the drag coefficient λ and the normal velocity $v_\perp$. The other terms are the pressure difference ΔP and the line tension γ.

the films (surface Plateau borders) sliding along the channel walls [26].

The majority of research to date has focused on quasi-static models of foam rheology (as outlined in Section 4), which fail to reproduce important effects observed in some high velocity experiments (see Section 4.5). We are thus motivated to improve upon these models by considering some of the viscous effects.

To meet these challenges, we use the so-called Viscous Froth Model, which is a dynamical model describing the evolution of 2D foams. It was introduced in the context of domain growth [28], and has since been used to simulate the dynamics of isolated topological events such as the relaxation of a foam system following a film rupture [16,27,29].

In order to demonstrate the model's predictive strength, we apply it to the example of foam flow around the U-bend, introduced in Section 4.5. It successfully reproduces the qualitative effects observed in the experiment. First steps to establishing a quantitative relationship between simulation and experiment deliver promising results, which we describe below.

5.1. The Viscous Froth Model

The Viscous Froth Model (Fig. 10) equates the forces (per unit length) acting at each point of a film separating two bubbles by

$$\Delta P - \gamma c + \lambda v_\perp^\alpha = 0. \tag{5.1}$$

This is an extension of the well-known Laplace equation [30] by a viscous term $\lambda v_\perp^\alpha$. ΔP is the difference between the gas pressures in the adjacent bubbles, γ the line tension (see Section 5.2), c the local curvature of the film and $v_\perp$ is its normal velocity. The coefficient of viscous drag is denoted by λ. Analysis of the flow of individual bubbles in tubes established $\alpha = 2/3$ [31], which is confirmed by recent work on quasi-2D foam flow by Cantat et al. [26] and Dollet et al. [32]. Current research finds a range of values for α between 1/2 and 2/3, seemingly dependent on the mobility of the interfaces of the foam [32–34].

Here we employ the "Linear Viscous Froth Model" by setting $\alpha = 1$. This allows for a much more tractable computational model as outlined in [16], while still capturing the essential viscous effects present in the system.

We implement the Viscous Froth Model in the Surface Evolver software [23]. The Surface Evolver is a natural choice as it provides all necessary book-keeping tools to keep track of the discretization of the film network and to determine the curvatures of the films. For a detailed discussion of our implementation see [16].

5.2. Example of the Viscous Froth: foam flow around a bend

We illustrate the power of the Viscous Froth Model by applying it to foam flow around the tight bend introduced in Section 4.5.

Simulations using the quasi-static model show no neighbor-switching process taking place in the U-bend, which is consistent with the low velocity experimental result. In this limit, the foam structure looks as shown on the left in Fig. 11, flowing around the bend without undergoing any topological changes. Upon increase of the velocity v, the viscous forces of the films being dragged along the top and bottom plate become of the order of magnitude of the surface tension force. Since the local velocity – and hence the viscous force – increases towards the outer boundary of the bend, an additional shear stress is imposed on the foam structure within the bend. For sufficiently high flow velocities this leads to a clearly visible distortion of the structure, as can be seen on the right in Fig. 11. Simulations applying the Viscous Froth Model reproduce this distortion very well (bottom row of Fig. 11).

At a critical velocity v_c the shortest film in the bend shrinks to zero length, triggering the neighbor-switching process, which is generally called a "T1" transformation. Before this

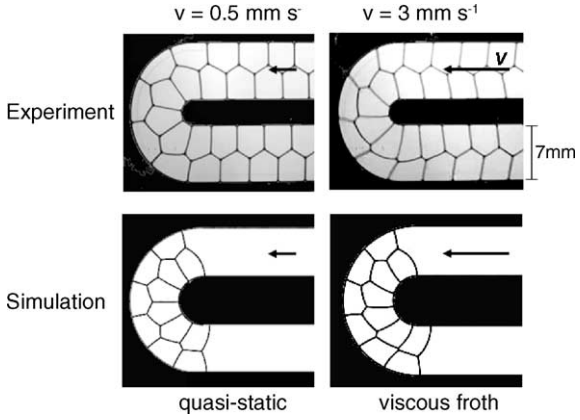

Fig. 11. Comparison of the distortion of a foam structure going around a bend without neighbor switching of bubbles (T1).

occurs, all cells have four interior films. Upon the flipping of the film two pairs of five- and three-sided cells are generated, of which one pair follows the foam flow and leaves the bend. The other one moves into the bend to release the stress. This new topology generates a succession of T1 processes for all the following bubbles (see Fig. 9).

As discussed in Section 4.5, this effectively shifts the two rows of bubbles with respect to each other by one bubble. For even higher velocities, the structure will again be increasingly stressed until another edge flips to give a second T1. This can be driven even further, with n T1 processes resulting in a phase shift of n bubbles between the two rows of bubbles.

With the Viscous Froth Model we can make a range of predictions about the behavior of the system as a function of various parameters, which can then be tested experimentally. One of the key quantities of interest in this problem is the critical velocity v_c as a function of various system parameters (e.g. bubble area, channel width and radius of curvature, liquid fraction, etc.).

The direct measurement of critical velocities of this nature in an experiment, however, are subject to significant errors. We therefore consider the length of the critical film (see Fig. 12). As the foam moves through the bend, the length of this film decreases and then increases again, going through a well defined minimum length L, which we measure as a function of the foam flow velocity v. We use very dry foams with a liquid fraction of less than 1%. v is increased very slowly to provide quasi-steady conditions. By doing this we can extrapolate to find v_c for $L \to 0$, and determine the drag coefficient λ by fitting the numerical prediction to the experimental data. This is possible because λ acts as a scaling parameter for the velocity in Eq. (5.1) ($\alpha = 1$).

The computer simulation of the U-bend uses the physical parameters of the experimental system: channel width = 7×10^{-3} m, inner channel radius = 1.5×10^{-3} m, bubble area = 1.86×10^{-5} m^2 and the line tension = 3×10^{-5} J/m. The line tension is the 2D analogue of the surface tension. It is estimated for our system by multiplying the surface tension of the solution (3×10^{-2} J/m^2) by the depth (0.5×10^{-3} m) of the channel, and by the factor 2 in order to account for the fact that each film consists of two interfaces. The drag parameter λ is replaced by an arbitrarily chosen $\lambda_{sim} = 1\,\mathrm{kg\,m^{-1}\,s^{-1}}$, and later determined by fitting the experimental and computational data. The foam is pushed around the bend at a range of velocities lower than v_c whilst keeping track of the minimum line length L_{sim} (Fig. 12).

The simulation data is fitted to a power law

$$L_{sim} = a v_{sim}^{b} + d, \tag{5.2}$$

using a, b and d as fitting parameters. We obtain values of $a = -1.26 \times 10^{-3}$ s, $b = 1.29 \times 10^{-3}$ and $d = 1.98 \times 10^{-3}$ cm. To estimate a value for λ we fit our experimental data with the function

$$L_{exp} = a(2\lambda v_{exp})^{b} + d \tag{5.3}$$

where the factor 2 takes into account the drag occurring on the top and bottom plates.

From this procedure we obtain the value of $\lambda \approx 14\,\mathrm{kg\,m^{-1}\,s^{-1}}$. Fig. 13 shows an example of experimental and simulation data, in which the latter was rescaled using the obtained λ parameter.

A direct comparison of this value with previous estimates for the viscous drag [31,26] is not straightforward. For example, using a different value of α in Eq. (5.1) changes λ. However, this estimate of λ will assist in the design of future experiments, which will also aim to establish a relationship between λ and the liquid fraction of the foam.

5.3. Further considerations

Despite the good agreement between experiment and simulation, there are some important aspects arising from this work which deserve more attention in attempting to test the potential and limitations of the Viscous Froth Model. We briefly illustrate the most important ones in the next sections.

5.3.1. Relaxation times

Viscous dissipation has a significant influence on how long it takes a 2D-foam to equilibrate [16]. In order to provide

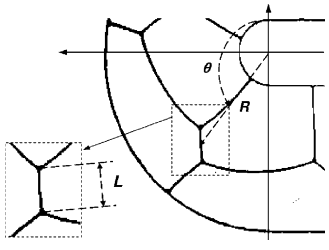

Fig. 12. We measure the shortest edge length L as a function of foam flow velocity v around the U-bend. If this edge gets short enough, a T1 neighbor switching process occurs.

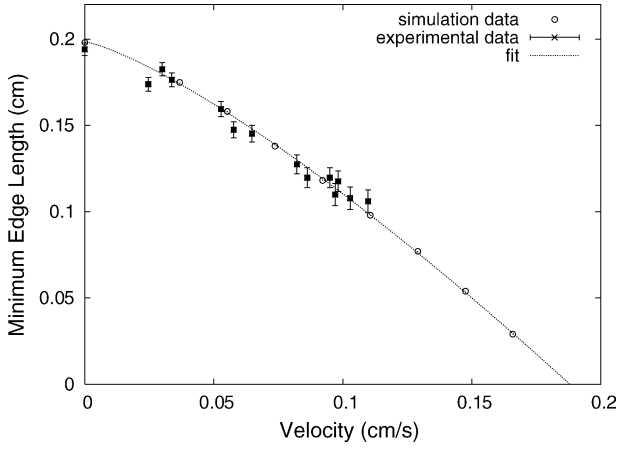

Fig. 13. Determination of the viscous drag parameter λ through fitting data from viscous froth simulations to the experimental results. The critical velocity is found to be $v_c = 0.19$ cm/s The minimum film length for zero velocity corresponds to the quasi-static simulation result.

quasi-steady conditions in experiments, it will be important to understand the magnitudes of the various time scales involved.

Fig. 14 shows an example of how measurements of the minimum film length L (introduced in the previous section) change, if the foam flow velocity v is increased too quickly. In series 2, v was increased more rapidly than in series 1, leading to significantly longer length L for the same velocity. We assign this to the fact that the foam velocity changed more quickly than the foam could equilibrate. Hence, we deal with "out of equilibrium processes", which seem important in the physics of foam flow and will have to receive much closer attention in future research.

5.3.2. Rules of equilibrium

The physics of dry 2D foams is governed by two important equilibrium rules [13]:

(1) films are arcs of circles, whose curvature is determined by the pressure drop across the edge;
(2) films meet each other three-fold at equal angles of 120° and they meet the container boundary at 90°.

For flowing foams in which viscous effects are important, it is obvious that (1) can not hold, as the drag force varies along a film, depending on its orientation to the flow direction.

Rule 2, however, is always obeyed for the infinitely dry foams employed in our simulations [16]. To see this, consider a small control area around a vertex which is subjected to the pressure, surface tension and drag forces imposed by the edges. If we now make the control volume infinitely small, only the surface tension forces remain. As they are equal for every edge, the angles between the edges must be equal, which gives 120° for interior vertices and 90° for vertices at the wall.

The experimental situation is more complex. The most striking deviation concerns the angles of vertices at the wall, which differ notably from 90° even for low foam flow velocities. The drier the foam, the more evident this becomes. Fig. 15 illustrates this effect for a dry and a wet staircase structure. The measurements are taken for the same channel cross-section (0.5 mm × 7 mm) and material used for the U-bend in Section 4.5. They seem to suggest a linear relationship between the angle deviation δ and the flow velocity of the foam, the slope depending on the liquid fraction.

Various factors may come into play here, examples being the finite size of the Plateau borders and vertices, or Marangoni effects [35]. The most important influence is expected from the viscous drag caused by Plateau borders sliding along the side walls and corners of the channel, which has not been included in the Viscous Froth simulations yet.

For the highest velocities considered here, it furthermore seems that the interior angles deviate from the 120°. For an example see Fig. 16. The word "seems" is used in this context because the precise angles at the vertex are very difficult to determine due to the curved nature of the edges.

In the present model, only normal forces acting on the edges are taken into account. Recent work by Cantat et al. [26] confirms that this is indeed a good approximation for dry foams at low foam flow velocities. At higher velocities, however, the liquid transport along the Plateau borders might contribute to a significant tangential viscous force. Unlike the normal force, this would have an effect on the angles at vertices, as it acts parallel to the surface tension force.

5.4. The future of modeling viscous effects in foams

Using the simple experimental setup of an ordered, quasi-two-dimensional foam structure flowing around a tight bend, we have been able for the first time to qualitatively and quantitatively test the predictive strength of the Viscous Froth Model. Even though these investigations are preliminary, we believe that the results given here already demonstrate the success of the Viscous Froth Model. Despite its simplicity,

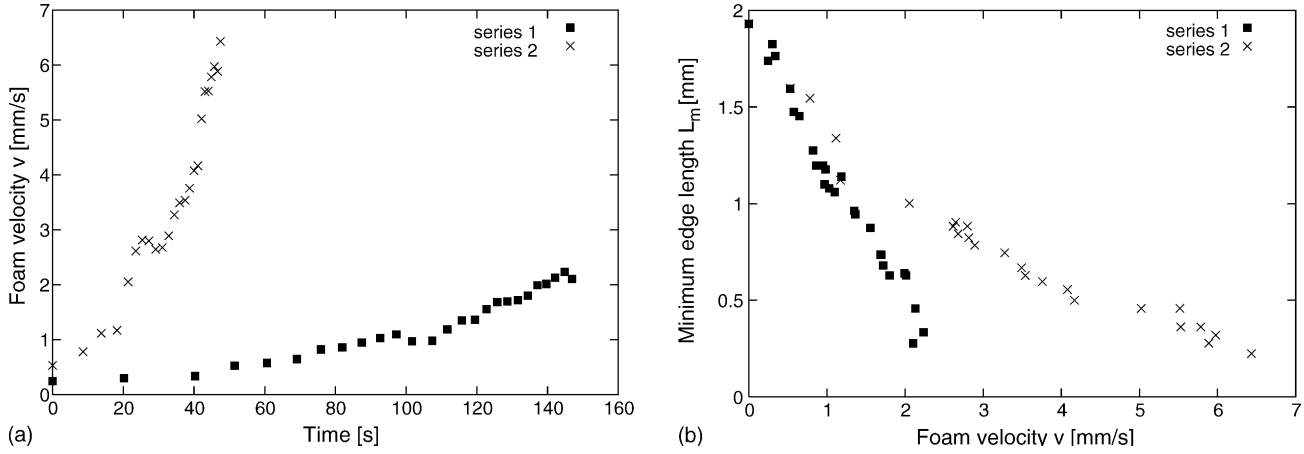

Fig. 14. The effect of a long relaxation time on a foam in a quasi-2D geometry: The variation of the minimum film length L with foam flow velocity v depends markedly on how quickly the foam is accelerated.

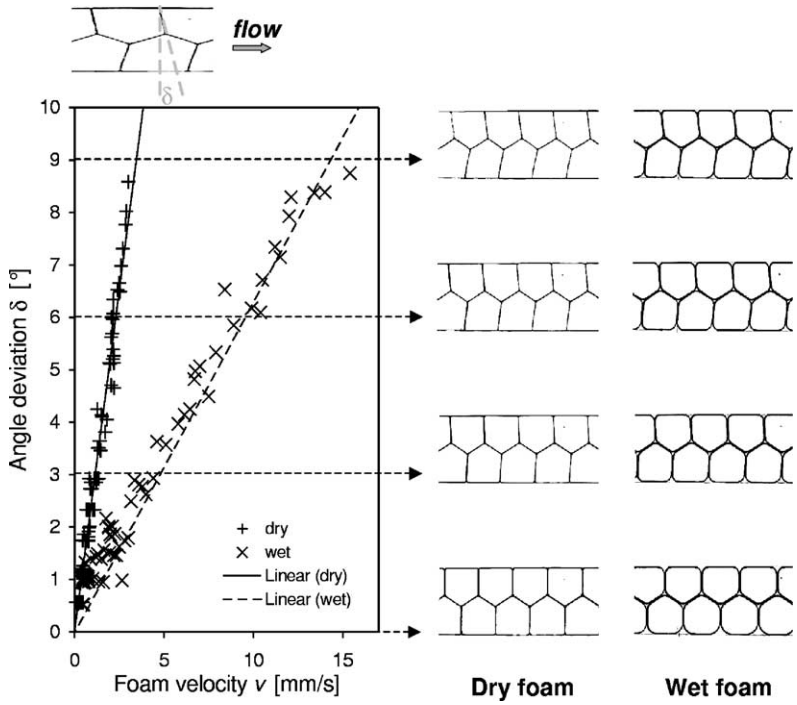

Fig. 15. The angles between films and channel walls deviate notably from the predicted 90°. This deviation δ increases very linearly with the foam flow velocity v. The slope depends significantly on the liquid fraction of the foam.

we find excellent agreement between experiments and simulations to the extent that we can employ the Viscous Froth Model to extract physical parameters like the viscous drag coefficient λ of a foam film sliding along a surface. It remains to be seen how this λ compares to similar experiments like those of Cantat et al. [26], keeping in mind that we have chosen $\alpha = 1$ in Eq. (5.1).

Above all, it will be important to understand the detailed nature of the dissipation mechanism, in particular the role of the bulk versus interface properties and the liquid fraction ϕ. Fortunately, modern research provides us with a vast range of liquids, surfactants and polymers to use as building blocks for thorough investigations of the individual parameters of interest. In this process it will be equally important to establish values for the exponent α in Eq. (5.1). The quantification of an appropriate 2D liquid fraction and its measurement, however, is still an open problem, which needs to be addressed in this process.

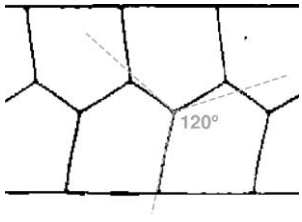

Fig. 16. For high flow velocities the interior angles of a 2D foam appear to deviate from the predicted 120°. Example: Plexiglas channel, width: 7 mm, depth: 0.5 mm, flow velocity $v = 15$ mm/s.

Understanding the precise interplay between λ and the various relevant system parameters should enable us to purpose-design channel elements on the computer using the Viscous Froth Model. For this and other purposes it will be necessary to establish quantitative criteria of the various approximations that can be applied in the modeling of the foam flow. Current research by Dollet et al. [32] indicates that the capillary number $\mathrm{Ca} = \eta v/\gamma$ (ratio of viscous and surface tension forces) by itself may not be a sufficient parameter, as originally expected. Their experiments show, for instance, that the foam velocity v and the liquid viscosity η have to be considered as independent parameters.

We have demonstrated some effects which cannot be accounted for within the Viscous Froth Model. It will be important to understand their significance in order to decide under which conditions they can be neglected or how they could be implemented into the existing model. Particularly important may be the implementation of additional drag conditions for the side walls. Guidance in the exploration of the true nature of the various effects may come from extensive research carried out on the motion of bubbles and bubble trains in tubes of various cross-sections [31,36–40,26].

Further questions arise regarding the dissipation of the T1 process itself. If a continuous pressure is applied to drive the foam through the channel, small pressure jumps should occur during a T1. Their magnitude would give information about the amount of energy dissipated in a T1 process. This may provide additional insights into the bulk dissipation in a foam.

6. Sample storage and analysis

Traditional microfluidic systems lack an efficient connection between the microfluidic chip, the micro-assay (well-plate) and sample storage. Our proposed technology solves this problem very naturally, as all three requirements can be accommodated and easily connected using the same technology, namely purpose-designed channel geometries on appropriate chips.

Possible examples are plentiful. An obvious geometry for a combined micro-assay and storage device, replacing traditional well plates, would be a serpentine channel containing a single column of samples structure. Fig. 17 shows an example of this type of device with two rows of samples in the channel. Another promising possibility may be to arrange a spiraling channel on a chip of conventional CD format. This would allow to built on the knowledge and technology already developed for traditional CD purposes.

If the channel system is sealed properly and diffusion between samples prohibited, the system can be stored for a very long time. These timescales depend on the chemistry of the system and could last up to weeks, months or even years [13].

7. Conclusions and outlook

In this paper we introduce a novel method of sample manipulation for microfluidic applications, based on the interaction between ordered sample structures and channel geometries. We have termed this technology Discrete Microfluidics.

We believe that the proposed method will have many advantages over current practice. It may not only solve several of the problems encountered in fluid or gas sample handling, but also has the potential to generate a plethora of exciting new possibilities of sample manipulation, analysis and storage. In an attempt to give an overview of the basic ideas of Discrete Microfluidics we could only touch on a few of these issues. Various aspects of the method will have to be thoroughly investigated in the future in order to explore the feasibility of the proposed technology for the vast range of possible applications in this field.

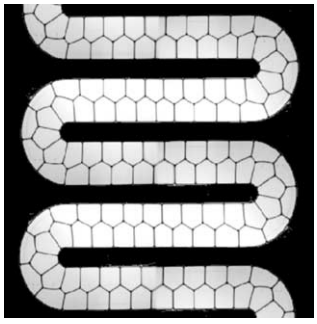

Fig. 17. Example of a channel arrangement which could be used for sample storage and analysis purposes.

Most importantly, we have to find out about possible problems entailed in down-scaling the proposed methods to the scales required by microfluidics. The generation of ordered foam structures in micro-channels has been successfully demonstrated by Garstecki et al. [18]. We would like to emphasize, however, that not every promising application requires microfluidic dimensions.

The investigation of various surfactants will become a key issue for chemically sensitive applications. Chemists have provided the research community with a broad range of surface active molecules (ionic and non-ionic), from which appropriate surfactants can be chosen. The food industry is a major driving force in developing foams and emulsions stabilized by particles instead of molecules.

An associated question is that of diffusion of chemicals between the samples. The continuous phase will have to be chosen very carefully to prohibit or reduce diffusion. In some cases, however, it might be of interest to allow a certain amount of controlled diffusion for mixing purposes.

For some applications it might be advantageous to use the continuous phase as sample material. The volume of the often expensive substances could then be reduced easily down to 0.5% of the channel volume, whilst keeping reasonably big channels.

The implementation of magnetic fluids and specifically designed magnetic fields adds an additional dimension of remote manipulation. We have demonstrated its usefulness for sample generation [15]. Using ferrofluids for the continuous phase allows to deform and twist sample structures, to provoke transitions between them and to locally vary the volume fraction using magnetic fields [14].

In our simple, large-scale geometries it is possible to move the sample structures by applying a pressure at the inlet of the channel system. For more complicated networks on smaller scales this will not be sufficient. Alternative methods will have to be developed. These could either be based on methods already used in continuous or digital microfluidics, or exploit some of the particular strength of the discrete nature of our system. Magnetic fluids, for instance, could be employed to drive the structures through the channels using traveling magnetic fields. For this purpose, the magnetic fluids could either constitute the continuous phase or a certain number of the dispersed samples. These magnetic droplets could easily be added to, and removed from, an existing structure using, for instance, the magic cross proposed in Section 4.4. Dielectric media in combination with electric fields might prove equally promising.

For future applications it will be essential to design methods for the controlled merging and splitting of samples. Using lasers to “pop” individual films between samples has proven very successful for foams [41]. The development of channel sections with adjustable wetting properties may be just as promising.

The minimization of interfacial energy and the forces associated with it could be utilized for various other aspects. One of the more obvious examples would be the design of

valves. If a channel geometry is designed such that the interfacial area of a structure increases or decreases more quickly by moving in one direction or another, it could potentially be used as a rectifier.

At some stage it may be interesting to consider bi-disperse or poly-disperse foam or emulsion structures to obtain well controlled ratios between sample volumes. Generation of these structures maybe realized, for instance, by employing traversing pins [42,43].

In the long run it would be useful to create dynamic channel designs, which can change shape to adjust to the required task. For instance, the "bump" in the switching element in Fig. 7(c) could be varied in shape depending on whether sample rows have to switch sides or not. Again, magnetic fluids might be a very promising candidate for this purpose.

In summary, we have introduced scientifically and commercially attractive tools for the handling of small liquid and gas samples. We have shown that these systems can be modeled successfully by taking advantage of quasi-static modeling (Section 4) and the Viscous Froth Model (Section 5) in the appropriate velocity ranges. We have been able to demonstrate the key features of these systems and are looking forward to exploring the vast landscape of scientific and applied opportunities opening up in front of us.

Acknowledgments

We would like to thank our summer student F. Richter for his support in the lab. K. Brakke's support on tricky Surface Evolver issues has been invaluable. This work benefited significantly from discussions with F. Graner, R. Seemann, S. Herminghaus, I. Cantat, R. Delannay, J. Osing and I. Shvets. Above all we would like to thank S. Hutzler and F. Elias for getting the ball rolling in the direction of Discrete Microfluidics. We are grateful for financial support from the Ulysses France-Ireland Exchange Scheme and the European Space Agency, Contract 14308/00/NL/SH (AO-99-031) CCN 002 MAP Project AO-99-075. W. Drenckhan was funded by the German National Merit foundation, G. Delaney by a Trinity College Award, and N. Kern by a Marie Curie European Fellowship (HPMF-CT-000-01079).

References

[1] Lab-on-a-Chip: The Revolution in Portable Instrumentation, 2nd ed., Wiley, 1997.
[2] Microfluidics Technology and Applications, Microtechnology and Microsystems Series, Research Studies Pr, 2000.
[3] N. Giorano, J.-T. Cheng, Microfluid mechanics: progress and opportunities, J. Phys.: Conds. Matter 13 (2001) R271–R295.
[4] L.J. Kricka, Microchips, microarrays, biochips and nanochips: personal laboratories for the 21st century, Clinica Chimica Acta 307 (2001) 219–223.
[5] F. Vinet, P. Chaton, Y. Fouillet, Microarrays and microfluidic devices: miniaturized systems for biological analysis, Microelectron. Eng. 61–62 (2002) 41–47.
[6] T. Chovan, A. Guttman, Microfabricated devices in biotechnology and biochemical processing, Trends Biotechnol. 20 (3) (2002) 116–122.
[7] S. Colin, Verrueckte fluide, Spektrum der Wissenschaft (2004) 46–50.
[8] D. Erickson, D. Li, Integrated microfluidic devices, Analytica Chimica Acta 507 (2004) 11–26.
[9] S. Mouradian, Lab-on-a-chip: applications in proteomics, Curr. Opin. Chem. Biol. 6 (2001) 51–56.
[10] B.H. Weigl, R.L. Bardell, C.R. Cabrera, Lab-on-a-chip for drug development, Adv. Drug Deliv. Rev. 55 (2003) 349–377.
[11] P. Tabeling, Some basic problems of microfluidics, Proceedings of the 14th Australasien Fluid Mechanics Conference, 2001.
[12] P. Paik, V.K. Pamula, R.B. Fair, Rapid droplet mixers for digital microfluidic systems, Lab on a Chip 3 (2003) 253–259.
[13] D. Weaire, S. Hutzler, The Physics of Foams, Clarendon Press, Oxford, 1999.
[14] S. Hutzler, D. Weaire, F. Elias, E. Janiaud, Juggling wih bubbles in cylindrical ferrofluid foams, Phil. Mag. Lett. 82 (2002) 297–301.
[15] W. Drenckhan, F. Elias, S. Hutzler, D. Weaire, E. Janiaud, J.-C. Bacri, Bubble size control and measurement in the generation of ferrofluid foams, J. Appl. Phys. 93 (12) (2003) 10078–10083.
[16] N. Kern, D. Weaire, A. Martin, S. Hutzler, S.J. Cox, The two-dimensional Viscous Froth model for foam dynamics, Phys. Rev. E. 70 (2004) 041411.
[17] R. Seemann, Private communication.
[18] P. Garstecki, I. Gitlin, W. DiLuzio, G.M. Whitesides, E. Kumacheva, H.A. Stone, Formation of monodisperse bubbles in a microfluidic flow-focussing device, Appl. Phys. Lett. 85 (13) (2004) 2649–2651.
[19] S. Hutzler, N. Peron, D. Weaire, W. Drenckhan, The foams/emulsion analogy in structure and drainage, Eur. Phys. J. E 14 (2004) 381.
[20] D. Weaire, S. Hutzler, N. Pittet, Cylindrical packings of foam cells, Forma 7 (1992) 259.
[21] N. Pittet, N. Rivier, D. Weaire, Cylindrical packing of foam cells, Forma 10 (1) (1995) 65–73.
[22] S. Hutzler, D. Weaire, R. Crawford, Moving boundaries in ordered cylindrical foam structures, Phil. Mag. B 75 (1997) 845.
[23] K. Brakke, The surface evolver, Exp. Math. 1 (1992) 141–156.
[24] M.E. Rosa, M.A. Fortes, Nucliation and glide of dislocations in a monodisperse two-dimensional foam under uniaxial deformation, Phil. Mag. A 77 (6) (1998) 1423–1446.
[25] ImageJ, http://www.rsb.info.nih.gov/ij/.
[26] I. Cantat, R. Delannay, N. Kern, Dissipation in foam flowing through narrow channels, Europhys. Lett. 65 (5) (2003) 726–732.
[27] S.J. Cox, D. Weaire, J.A. Glazier, The rheology of two-dimensional foams, Rheol. Acta 43 (2004) 442–448.
[28] D. Weaire, S. McMurry, Some fundamentals of grain growth, Solid State Phys. 50 (1996) 1.
[29] S.J. Cox, A viscous froth model for dry foams in the surface evolver, in: Proceedings of the Eufoam 2004, Coll. Surf. A 263 (2005) 81–89.
[30] P.S. Laplace, Mécanique Céleste, 1906. supplement to Book 10.
[31] F.P. Bretherton, The motion of long bubbles in tubes, J. Fluid Mech. 10 (1961) 166.
[32] B. Dollet, F. Elias, C. Quilliet, A. Huillier, M. Aubouy, F. Graner, Two-dimensional flows of foams: drag exerted on circular obstacles and disspiation, in: Proceedings of the Eufoam 2004, Coll. Surf. A 263 (2005) 101–110.
[33] N. Denkov, Private communication, 2004.
[34] R. Delannay, Private communication, 2004.
[35] C. Marangoni, Ueber die ausbreitung der tropfen einer fluessigkeit auf der oberflaeche einer anderen, Annu. Phys. (Leipzig) 143 (1871) 337–354.
[36] L.W. Schwartz, H.M. Princen, A.D. Kiss, On the motion of bubbles in capillary tubes, J. Fluid Mech. 172 (1986) 259–275.
[37] J. Ratulowski, H.-C. Chang, Transport of gas bubbles in capillaries, Phys. Fluids A 1 (10) (1989) 1642–1655.
[38] H. Wong, C.J. Radke, S. Morris, The motion of long bubbles in polygonal capillaries. Part 1. Thin films, J. Fluid Mech. 292 (1995) 71–94.

[39] H. Wong, C.J. Radke, S. Morris, The motion of long bubbles in polygonal capillaries. Part 2. Drag, fluid pressure and fluid flow, J. Fluid Mech. 292 (1995) 95–110.
[40] A.L. Hazel, M. Heil, The steady propagation of a semi-infinite bubble into a tube of elliptical or rectangular cross-section, J. Fluid Mech. 470 (2002) 91–114.
[41] I. Cantat, R. Delannay, Dynamical transition induced by large bubbles in two-dimensional foam flows, Phys. Rev. E 67.
[42] M.A. Fortes, J.M. Albuquerque, Two-dimensional foam fragmentation produced by traversing pins, Phil. Mag. A 81 (9) (2001) 2217–2232.
[43] J.M. Albuquerque, M.A. Fortes, Foam patterning by traversing pins, Phil. Mag. A 81 (9) (2001) 2233–2241.